INSTITUTE OF PHYSICS PUBLISHING JOURNAL OF OPTICS A: PURE AND APPLIED OPTICS

J. Opt. A: Pure Appl. Opt. **6** (2004) 193–203 PII: S1464-4258(04)68520-5

A new model of geometric chirality for two-dimensional continuous media and planar meta-materials

A Potts[1,2,3], D M Bagnall[1,2] and N I Zheludev[1]

[1] School of Physics and Astronomy, University of Southampton, Highfield, Southampton SO17 1BJ, UK
[2] School of Electronics and Computer Science, University of Southampton, Highfield, Southampton SO17 1BJ, UK

E-mail: ap@ecs.soton.ac.uk

Received 4 September 2003, accepted for publication 12 November 2003
Published 24 November 2003
Online at stacks.iop.org/JOptA/6/193 (DOI: 10.1088/1464-4258/6/2/007)

Abstract
We have, for the first time, identified ten tenets of two-dimensional (2D) chirality that define and encapsulate the symmetry and scaling behaviour of planar objects and have used them to develop three new measures of geometric 2D chirality. All three models are based on the principle of overlap integrals and can be expressed as simple analytical functions of the two-dimensional surface density, $\rho(\mathbf{r})$. In this paper we will compare the predicted behaviour of these models and show that two of them are fully integrable and scalable and can therefore be applied to both discrete and continuous 2D systems of any finite size, or any degree of complexity. The only significant difference in these two models appears in their behaviour at infinite length scales. Such differences could, however, have profound implications for the analysis of chirality in new generations of planar meta-materials, such as chiral arrays, fractals, quasi-periodic 2D crystals and Penrose tiled structures.

Keywords: chiral, planar geometry, optical activity, overlap integral, 2D topology

1. Introduction

The importance of planar chirality in optics was probably first highlighted by Hecht and Barron [1], who theoretically evaluated the polarization sensitivity of incoherent light scattered from ensembles of planar chiral molecules. Recent experiments investigating the optical properties of planar chiral media [2, 3] have now shown that two-dimensional (2D) chiral objects with characteristic sizes $\sim$2 μm are also capable of manipulating the polarization state of coherent light. In particular, it was found that linearly polarized light in the visible and infrared regions of the spectrum experiences azimuth rotation and elliptization when diffracted from arrays of gammadion-shaped chiral holes that are etched into a thin metallic film and supported on a silicon substrate. These polarization changes were strongly correlated to the degree of chirality of the gammadions and were found to reverse sign when the handedness of the gammadions was reversed. Similar effects had previously been predicted for significantly larger metallic gammadions in the microwave regime [4].

It is now clear that composite planar materials whose properties (such as 2D chirality) are artificially engineered on the nano-scale (so-called meta-materials) could herald new opportunities for novel devices in opto-electronics, while nano-structured chiral surfaces could also exhibit strong enantiomer-specific behaviour that would be of considerable interest in many areas of chemistry [5, 6]. However, in order for the chiral properties of these various artificial planar materials to be designed more efficiently, a quantifiable measure of 2D chirality is required. Over the last fifteen years there has been significant progress in this area, but most of this work has been

[3] Author to whom any correspondence should be addressed.

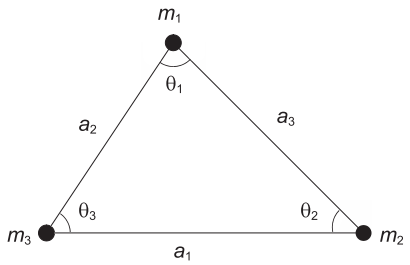

Figure 1. The labelling convention used for the sides, vertices and angles of a triangle.

driven by the needs of stereochemists. As a consequence, the resulting chiral measures tend to be more applicable to microscopic systems of discrete points [7–10] where the points themselves are usually taken to represent the spatial positions of atomic nuclei, whether in molecules or on planar surfaces.

Unfortunately, most of the discrete chirality measures that have so far been proposed are not easily extendible to macroscopic systems. One reason for this is that the spatial distribution of mass in macroscopic systems is best described by a continuous distribution function, $\rho(\mathbf{r})$ (where $\rho(\mathbf{r})$ represents the local density of point masses and is, in effect, a two-dimensional mass density function for that surface), rather than a set of spatially isolated discrete points. Secondly, the methodologies (such as group theory [8, 9] and optimized overlap integrals [10]) that these discrete 2D chiral models employ become increasingly difficult or cumbersome to implement as they are applied to larger and larger systems. Attempts to simplify complex structures by considering only the 'most significant' points in a structure [9] can also be problematic as it may not always be obvious which points are the most significant. What most experimenters desire is an algebraic formulation of the theory of 2D chirality that can be applied to any 2D mass distribution (discrete or continuous) simply by summing (or integrating) the chirality function over the density distribution function, $\rho(\mathbf{r})$.

One of the first (and most promising) algebraic models to incorporate continuous mass distributions was developed by Osipov *et al* [11]. They pointed out that the simplest chiral object in two dimensions is a scalene triangle and, consequently, if one can construct a chirality measure for this simple set of three points, it then becomes a trivial exercise to extend the measure to any larger distribution of points merely by summing over all possible triangular permutations. By employing this approach they derived an expression for the chirality of a single triangle of points:

$$K = \frac{\Delta}{(a_1a_2a_3)^2}\left[\left(\frac{a_1^2}{a_3^2}-\frac{a_1^2}{a_2^2}\right)\cos(\theta_1) + \left(\frac{a_2^2}{a_1^2}-\frac{a_2^2}{a_3^2}\right)\cos(\theta_2) + \left(\frac{a_3^2}{a_2^2}-\frac{a_3^2}{a_1^2}\right)\cos(\theta_3)\right]. \quad (1)$$

Here, a_1, a_2 and a_3 are the lengths of the three sides of the triangle while θ_1, θ_2 and θ_3 are the angles opposite to sides a_1, a_2 and a_3, respectively. The term Δ is the triangle's area. By convention, we usually number all vertices, sides and angles of the triangle in a clockwise direction, as shown in figure 1.

The model of Osipov *et al* clearly satisfies many requirements for a truly universal macroscopic model of 2D chirality. It changes sign under enantiomeric inversion, while $K = 0$ for any isosceles or equilateral triangle, or when the three points are co-linear. Unfortunately, it also has three main failings. The most serious is its behaviour in the limit of converging points. The expression for the chirality of a set of three points in equation (1) clearly diverges as the length of any side of the triangle tends to zero and, consequently, it is not integrable unless a cut-off parameter is introduced. Secondly, its scaling behaviour is inappropriate, with K actually decreasing as the size of the object increases. The final drawback of this model is that it is not founded on purely geometric principles, unlike most other recent 2D chirality models [8–10], but also involves the incorporation of electromagnetic polarization effects through the interaction of induced dipoles situated at each vertex of the triangle. Such an approach tempers the generality of the model and its potential applications. More fundamentally, however, such an approach can also introduce unwanted confusion into the definition of chirality. Chirality and optical activity are not synonymous. One is cause, while the other is effect; and the absence of one is not necessarily proof of the absence of the other. Nor do they necessarily scale proportionately. In analysing two-dimensional chirality we are trying to formulate a theory of asymmetry based purely on geometric arguments that can be applied universally, irrespective of the material nature of the system.

In this paper we will present a new measure of 2D chirality (K), based on purely geometric considerations, that is scalable and integrable and that is capable of being applied to any generalized continuous distribution, $\rho(\mathbf{r})$, for any 2D surface. Our starting point will be to define a chirality measure for a triangular set of points based on asymmetry in the area of that triangle. We will present three possible methodologies for achieving this, but will argue that an angular bisection method (see section 6) is the only one of the three that fully satisfies all the conditions that we require. We will then extend this measure to larger structures by summing the chirality measure over all possible permutations of triangles in a manner similar to the methodology of Osipov *et al* [11]. In addition, we will for the first time address the issue of scaling behaviour in 2D chiral systems. We will argue that for any triangular set of points there must be a chirality measure (Γ) that is independent of the magnification of the structure and is therefore dimensionless. We will then argue that a necessary condition for integrability of our chirality measure, K, is that it must scale with the area and mass of the system. Finally, we will outline the utility of our new model by demonstrating its ease of use and its consequences. We will also compare its theoretical results with those derived using other models, as well as with the results of recent optical experiments [2, 3].

2. Basic principles of chirality in 2D

The definition of chirality has changed little since it was proposed by Lord Kelvin over a hundred years ago [12]. An object is said to be chiral if it cannot be brought into congruence with its enantiomeric, or mirror image, form. This definition of chirality is related to the concept of parity and is only applicable to systems where the positions of the particles are time-invariant, although Barron has recently extended this definition to include time reversality [13]. Unfortunately, these

definitions of chirality are still insufficient as they actually represent a reconstitution of the definition of symmetry, or achirality. The main drawback of defining chirality in this way, as a negative concept, is that it implies that chirality is a state variable with only two possible outcomes; chiral (true) and achiral (false). Recently, though, Le Guennec [14] has shown that in two dimensions chirality is, in fact, a continuous measure and, consequently, it should be possible to express it as a continuous function.

In two dimensions, the chirality measure itself is usually defined in one of two ways [7, 8]. The chirality index of the first kind is defined in terms of the minimum distance separating points in a chiral object from those in their closest achiral form, while the chirality index of the second kind is defined in terms of the minimum distance separating a point from the equivalent point in its enantiomer. It should be noted though that the symmetry operations required to generate the enantiomer are different in 2D and 3D. In three dimensions the enantiomeric form of an object is usually generated by a spatial inversion operation $\mathbf{r} \Rightarrow -\mathbf{r}$ (i.e. $x \Rightarrow -x$, $y \Rightarrow -y$, $z \Rightarrow -z$). This is also true in any other n-dimensional system provided n is odd. However, when n is even (such as in the two-dimensional case we will consider here), spatial inversion results only in spatial rotation and translation of the original object. The more general requirement for enantiomeric transformation is for spatial reflection through a hyperplane of dimension $n-1$. This is true for any n-dimensional system, whether n is odd or even. For a 2D object, this transformation equates to reflection of the object through any line in the plane (e.g. $x \Rightarrow -x$ or $y \Rightarrow -y$, but not both).

As discussed in the previous section, the simplest chiral object in two dimensions is defined by a set of three points. However, as any complex pattern or feature of finite extent can be described by a larger set of N such points, it should be possible to calculate the chiral index, K, simply by summing over all the contributions arising from every possible subset of three points. Thus, if we can construct a measure of chirality for a three-point set (in other words a triangle) then we can extend the theory to any structure, with any degree of complexity, in a manner similar to that described previously by Osipov *et al* [11]. It should be noted, however, that such an approach is inherently non-linear as the number of possible permutations scales as N^3 (for large N) rather than as N (where N is the number of points or pixels defining the size of the system), but this is entirely consistent with the behaviour of chirality. Chirality does not scale linearly. A system of N identical chiral objects does not necessarily possess N times the amount of chirality of a single object. The difference is due to additional chirality arising from how the individual objects are arranged on a lattice (which may or may not be periodic), and therefore scales with the size and degree of complexity of that lattice. The contribution to K arising from this arrangement we term structural chirality (as opposed to molecular or elemental chirality, which is the intrinsic chirality of an individual element). In order to formulate a measure of chirality in 2D we need to start by outlining a set of conditions that we believe should underpin any potential theory and define the required behaviour of the chirality index. Once these conditions are set we will attempt to define the theory of chirality itself for a single triangle and thence to its generalized form.

In two dimensions the basic chiral element is the triangle. The chirality index (K) of any set of N points ($N > 3$) can be derived, therefore, by summing the chirality indices of all possible permutations of triangles. This then leads to our first condition.

Postulate 2.1. If we define K_{ijk} as the chirality index of a triangular set of points $\{\mathbf{r}_i, \mathbf{r}_j \text{ and } \mathbf{r}_k\}$, then

$$K = \tfrac{1}{6} \sum_{i=1}^{N} \sum_{j=1}^{N} \sum_{k=1}^{N} K_{ijk}. \tag{2}$$

Lemma 2.2. *The chirality index of any triangle (K_{ijk}) must be proportional to the mass at each vertex, i.e.*

$$K_{ijk} = m_i m_j m_k \Lambda_{ijk} \tag{3}$$

where m_i, m_j and m_k are the masses at each of the three vertices defined by the set of 2D vectors $\{\mathbf{r}_i, \mathbf{r}_j$ and $\mathbf{r}_k\}$ and Λ_{ijk} is another chiral function that depends only on the spatial positions of the points i, j and k. Because Λ_{ijk} is a massless chirality measure, we refer to it as the specific chirality index. The term 'mass' referred to above is a two-dimensional quantity. In mathematical terms, it represents the total number of point masses at a given point or in a given area and is therefore equivalent to the integral of the 2D density distribution function, $\rho(\mathbf{r})$, over that area. In physical terms, where the 2D chiral structure may be a patterned thin film of varying thickness similar to those studied previously [2, 3], the mass can be thought of as the integral of the 2D mass density, $\rho_{2D}(\mathbf{r})$, over a given area. The 2D mass density is then just the product of the material density of the film, ρ (=19.3 g cm^{-3} for gold), and the film thickness at that point, in which case the mass term will have units of kilograms.

The proof of lemma 2.2 is trivial and goes as follows. Suppose we start with a set of three point masses that form a triangular set, as depicted in figure 1, but we then decompose one of the point masses (m_1, say) into a set of p coincident smaller point masses $\{m_{1q}\}_{q=1\ldots p}$ such that the total mass at point 1 (and hence of the system as a whole) is conserved. Now suppose we sum the chirality index over every possible permutation of triangles defined by the new set of points (m_2, m_3 and the set $\{m_{1q}\}_{q=1\ldots p}$), while assuming that all triplet sets of points that contain either two or three coincident points make no contribution to the chirality (see lemma 2.9). We can see that the value of K in equation (2) will remain unchanged only if K_{ijk} is proportional to the mass at each vertex, as indicated in equation (3). This condition is one of the criteria that is essential in order to ensure that the chirality index that arises as a result of equation (2) is independent of how the mass at any point is subdivided. It is therefore one of the essential criteria required to ensure integrability of the chirality function.

Postulate 2.3. The chirality index should be continuous and single-valued.

Lemma 2.4. *The chirality index cannot be dimensionless but must decrease in magnitude as the size of the structure decreases. The necessity for such behaviour can be understood by considering the following scenario. Suppose we take a single point mass and decompose it into three smaller, and*

spatially separated, point masses (m_1, m_2 and m_3), as shown in figure 1. Let us also impose the condition that the triangle of points that we form as a result of this procedure is scalene. The chirality index should now be non-zero. Now suppose we reverse the decomposition process so that the three points of the triangle converge to form the original single point mass, but do so subject to the condition that the angles of the triangle remain unchanged by the convergence. If the chirality index is dimensionless (as proposed by Solymosi et al [15] for the 3D model of Osipov et al [16]) then, as we perform this operation, the chirality index will remain non-zero, even as the three points converge to form a single point. But, by symmetry, a single point is achiral and postulate 2.3 forbids any discontinuity in the chirality index. Hence we have a paradox. This paradox can only be resolved if the chirality index contains a term that is dependent on the magnification of the set of points and hence on the actual area of each triangle. Only then will the contributions to the chirality index from infinitesimally small triangles vanish completely. The most obvious scaling function to choose is one that varies linearly with area.

Postulate 2.5. If the chirality index scales linearly with the area of the triangle Δ_{ijk}, any two triangles that are similar (i.e. their corresponding angles are identical) should have chiral indices that are proportional. Consequently it should be possible to define a dimensionless chirality index, Γ_{ijk}, that is a function of the ratios of the sides of the triangle or its three angles, but is independent of its area, Δ_{ijk}. By combining equation (3), lemma 2.4 and postulate 2.5 we can conclude that

$$K_{ijk} = m_i m_j m_k \Lambda_{ijk} = m_i m_j m_k \Gamma_{ijk} \Delta_{ijk}. \qquad (4)$$

Postulate 2.6. The dimensionless chirality index, Γ_{ijk}, must always be finite. This condition is required to ensure that the chirality index, K, of a finite system is always finite.

Postulate 2.7. The chirality index must be inverted under any reflection operation, i.e. as $x \Rightarrow -x$, $K \Rightarrow -K$. As the area of the triangle will remain unchanged by such an operation, then it is also true that $\Gamma_{ijk} \Rightarrow -\Gamma_{ijk}$ for the same reflection operation. Thus K and Γ_{ijk} are both zero for any isosceles or equilateral triangle.

Lemma 2.8. *The chirality index of any set of three co-linear points must be zero. This is satisfied if Γ_{ijk} is finite for a co-linear set (as $\Delta_{ijk} = 0$).*

Lemma 2.9. *If any two points of a triangle are coincident in space then the chirality index must be zero. This is a consequence of postulate 2.6 and implies that $K_{ijk} \to 0$ as $|\mathbf{r}_{ij}| \to 0$, where $|\mathbf{r}_{ij}|$ is the length of any side of the triangle. Expressions for K that fail to satisfy this condition (such as equation (1), for example) will diverge upon integration.*

Starting from this set of conditions, we will now attempt to construct a measure for Λ_{ijk} and hence for K.

3. Construction of the chirality measure using overlap integrals

In the previous section we argued that the specific chirality index for a triangular set of points (Λ_{ijk}) should have the dimensions of area (see equation (4) and postulate 2.5). It therefore follows that, when attempting to construct a mathematical definition for Λ_{ijk}, the crucial criterion is the degree of asymmetry in the distribution of that area. How we choose to assess this degree of asymmetry will ultimately determine the form and behaviour of the chirality index (K) itself.

In 2D the chirality index of a set of discrete points is usually determined by comparing the position of each point with an equivalent point in a non-chiral object (the chirality index of the first kind) or one in its enantiomeric set (the chirality index of the second kind). Of the two methods, the chirality index of the first kind is the most difficult to implement, as it involves the creation of an achiral set of points that is closest in form to that of the original chiral set [9]. This usually involves the application of different combinations of group symmetry operations (such as duplication, reflection through a plane, rotation, translation, etc) to each point in the original set individually, until an achiral set is formed. Clearly, as the size of the original set increases so, in general, does the number of symmetry operations. A secondary problem is that it is not clear that there is always a unique outcome for this generation process. In fact, the generation process may be degenerate with the creation of multiple equivalent, but different, achiral sets being possible. This problem of degeneracy will inevitably increase if the size of the original set is increased.

The chirality index of the second kind, in contrast, is relatively simple to implement. All that is required is the generation of the enantiomeric set, and for that a simple inversion operation (i.e. reflection through a 1D hyperplane) will suffice. Because only one symmetry operation is performed, and is performed simultaneously on all points in the original set, there can be no ambiguity or discretion in how it is applied and therefore no degeneracy of the final outcome. It is therefore clear that, of the two methods, the chirality index of the second kind is superior in terms of its ease of use and its uniqueness.

In order to formulate our desired measure of chirality of the second kind, we need to compare the asymmetry in the distribution of the area of our original triangle and its enantiomer. The simplest way to do this is to superimpose the two triangles and measure the amount of common area that they share. This is the concept of the overlap integral. Unfortunately, the magnitude of the common area will be determined by the relative translation and rotation of the two triangles. So, how do we arrive at a unique result for the overlap integral? One way is to determine the maximum overlap of the original triangle and its enantiomer (see figure 2(b)). This inevitably involves an optimization process, with the relative translation (in x and y) and rotation of the enantiomer being the three fitting variables. In fact, it is easy to see that there are only two free parameters (the perpendicular separation and the rotation) as the state of maximum overlap must have a plane of symmetry [7] (the broken line in figure 2(b)). We can then define the specific chirality index, Λ_{ijk}, as the area of those parts of the enantiomeric triangle that are not superimposed on any part of the original triangle in a manner similar to other authors [10]. We call this total area the antisymmetric area, Δ_{A}.

Unfortunately, while this method yields a magnitude for Λ_{ijk}, it does not define a unique sense or handedness for the

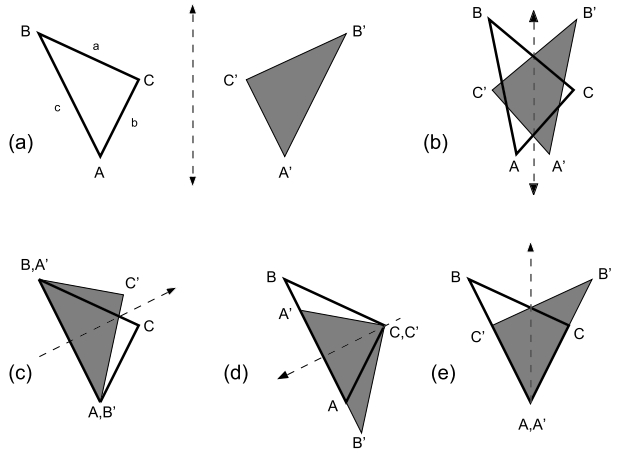

Figure 2. An illustration of the method of overlap integrals for triangles. (a) The original triangle (white) with its vertices and sides labelled and its enantiomer (shaded). (b) The condition of maximum overlap. The dotted line is the mirror plane, the arrowheads indicating spatially equivalent directions of view. (c) The perpendicular bisection method. (d) The coincident vertex, perpendicular intercept method. (e) The angular bisection method.

chirality. This is indicated by the two arrows on the mirror plane (broken line) in figure 2(b). Suppose we define the handedness to be the difference in areas of the original triangle across the mirror plane and arbitrarily choose the area to the right-hand side of the mirror plane to have a positive sense (the area to the left thus being negative). The two arrows on the mirror plane indicate that an observer has two possible definitions as to which side is the right and which is the left, both of which are geometrically equivalent. Hence the handedness is ambiguous because the definition of left and right cannot be applied consistently between triangles.

In order to eliminate this problem we need to define the mirror plane with an unambiguous direction. One way to achieve this is to pre-set the direction of the mirror plane relative to our chiral object. In order for such a direction to be non-arbitrary, however, it must represent a line of high symmetry for the triangle, but because the triangle will typically be chiral, this will not be possible, except in exceptional circumstances (i.e. for isosceles and equilateral triangles). However, the mirror plane can be a symmetry plane for a sub-set of points and sides of the triangle. Three such possibilities are shown in figures 2(c)–(e). What distinguishes these three arrangements is that they are the only ones that map more than one point and/or side onto another point or side of the enantiomeric triangle. As such, they represent the three highest symmetry arrangements attainable. The configuration in figure 2(c), for example, is the only one that maps two points onto each other, as well as mapping the adjoining side onto itself. In figure 2(d) point C is mapped onto itself, as is the opposite side of the triangle, whereas in figure 2(e) point A is again mapped onto itself while sides b and c of the triangle are mapped onto each other. In all these cases the mirror plane itself is asymmetric (as denoted by the single arrowhead) because it has a unique direction due to the way it is defined relative to the body of the triangle. Hence the handedness is now unambiguous and can be applied consistently for different triangles. However, because the triangle has three sides (and three vertices) that are all spatially equivalent, the process for calculating the chirality in figures 2(c)–(e) must be repeated for each side (or vertex) and the results combined so that the resulting total represents the chirality of the whole triangle and not the arbitrary value from only one viewpoint.

In the following sections we will calculate the chirality index using each of the symmetry arrangements shown in figures 2(c)–(e) and compare their results with previous models and the list of conditions set out in section 2.

4. The perpendicular bisection method

In the symmetry model illustrated in figure 2(c) the mirror plane is oriented so that it bisects one side of the triangle. We can now define the chirality index as the difference in areas subtended by our original triangle (the white triangle in figure 2(c)) across the mirror plane. The sense of chirality is arbitrarily, but consistently, chosen such that positive areas (Δ_{R}) lie to the right of the mirror plane (as seen by an observed standing at the intersection of the mirror plane and the side of the triangle it bisects and looking into the body of the triangle) and negative areas (Δ_{L}) to the left. The difference in areas is equivalent to the antisymmetric area, Δ_{A}, and gives the specific chirality index for that side (let us call it side 1) as follows:

$$\Lambda_1 = \Delta_{\mathrm{R}} - \Delta_{\mathrm{L}} = \Delta_{\mathrm{A}}. \tag{5}$$

It can be shown that Λ_1 is given by

$$\Lambda_1 = \frac{a_2^2 - a_3^2}{a_1^2 + |a_2^2 - a_3^2|}\Delta \tag{6}$$

where Δ is the area of the triangle and the side lengths a_1, a_2 and a_3 are defined in a clockwise fashion, as illustrated in figure 1. If we repeat this procedure for sides 2 and 3 of the triangle (but using a different mirror plane for each case) we will arrive at the following results:

$$\Lambda_2 = \frac{a_3^2 - a_1^2}{a_2^2 + |a_3^2 - a_1^2|}\Delta \tag{7}$$

and

$$\Lambda_3 = \frac{a_1^2 - a_2^2}{a_3^2 + |a_1^2 - a_2^2|}\Delta. \tag{8}$$

For arbitrary values of a_1, a_2 and a_3 equations (6)–(8) will each give a different result for the specific chirality index, all of which are of equal merit. We therefore define the total specific chirality index for the triangle as the sum of the three terms:

$$\Lambda_{ijk} = \Lambda_1 + \Lambda_2 + \Lambda_3. \tag{9}$$

The justification for this is that, when we extend this model to larger systems, we calculate the chirality index by summing over all possible triangular permutations (see postulate 2.1) and hence over all possible permutations of mirror planes. Therefore, it seems logical to do the same for each mirror plane within each triangle. However, it should be noted that Buda *et al* [10] have proposed a method of chirality products for their 2D chirality measure.

By applying postulate 2.1 we can now write the total chirality index of the system as

$$K = \tfrac{1}{4}\sum_{i=1}^{N}\sum_{j=1}^{N}\sum_{k=1}^{N} m_i m_j m_k \times \frac{|\mathbf{r}_{ij}|^2 - |\mathbf{r}_{ik}|^2}{|\mathbf{r}_{jk}|^2 + ||\mathbf{r}_{ij}|^2 - |\mathbf{r}_{ik}|^2|}(\mathbf{r}_{ij} \times \mathbf{r}_{ik}) \quad (10)$$

where $\mathbf{r}_{ij} = \mathbf{r}_j - \mathbf{r}_i$, $\mathbf{r}_{ik} = \mathbf{r}_k - \mathbf{r}_i$ and the cross-product $\mathbf{r}_{ij} \times \mathbf{r}_{ik} = 2\Delta_{ijk}$. The additional prefactor of $1/2$ is required to compensate for double counting of triangles by the triple summation. Inspection of equations (6)–(10) shows that this model for the specific chirality index satisfies all of the conditions laid down in section 2. It changes sign under enantiomeric inversion and the dimensionless chirality index is always finite. Thus the chirality index of a triangle, K_{ijk}, is zero when the three points of the triangle are co-linear or when any two points are coincident. However, as we shall see, the perpendicular bisector model is not the only model that satisfies our list of postulates and lemmas.

5. The perpendicular intercept method

If one were to envisage the purest form of chiral triangle one would probably think of a scalene right-angled triangle. Therefore, if we could deconstruct any triangle into two such right-angled triangles, one left-handed and one right handed, we could then use the difference in areas of these triangles as our measure of chirality. This approach is illustrated in figure 2(d) where, starting at one vertex, a perpendicular line is drawn to the opposite side of the triangle that intercepts that side at right-angles and splits the initial triangle into two distinct right-angled triangles. We then define Γ_1, the dimensionless chirality index for vertex 1, as the difference in areas divided by the total area. The sense of chirality is again arbitrarily chosen such that positive areas (Δ_R) lie to the right of the mirror plane (this time as seen from the vertex) and negative areas (Δ_L) to the left, so that the final form for Γ_1 is as follows:

$$\Gamma_1 = \frac{\Delta_R - \Delta_L}{\Delta_R + \Delta_L} = \frac{a_2\cos(\theta_3) - a_3\cos(\theta_2)}{a_1}. \quad (11)$$

The side lengths a_1, a_2 and a_3, and the angles θ_2 and θ_3 are again defined in a clockwise fashion as illustrated in figure 1.

If we repeat this process for vertices 2 and 3 we arrive at the following expression for the dimensionless chirality index for a triangular set of points, Γ_{ijk}:

$$\Gamma_{ijk} = \left(\frac{a_3}{a_2} - \frac{a_2}{a_3}\right)\cos(\theta_1) + \left(\frac{a_1}{a_3} - \frac{a_3}{a_1}\right)\cos(\theta_2) + \left(\frac{a_2}{a_1} - \frac{a_1}{a_2}\right)\cos(\theta_3) \quad (12)$$

and, if we use the cosine rule to substitute for the angles θ_1, θ_2 and θ_3 in terms of the sides a_1, a_2 and a_3, we find that

$$\Gamma_{ijk} = \left(\frac{a_2^2}{a_1^2} - \frac{a_1^2}{a_2^2}\right) + \left(\frac{a_3^2}{a_2^2} - \frac{a_2^2}{a_3^2}\right) + \left(\frac{a_1^2}{a_3^2} - \frac{a_3^2}{a_1^2}\right). \quad (13)$$

It can be seen that equations (12) and (13) are both similar in form to the equation derived by Osipov *et al* (see equation (1)). As such, they satisfy most of the conditions outlined in section 2, particularly the spatial reflection criterion outlined in postulate 2.7, but crucially they do not satisfy postulate 2.6 nor lemma 2.9. The reason for this can be understood by considering the behaviour of the triangle illustrated in figure 1 as one side of the triangle is maintained at a constant length, a_1, while a second side (a_2) is gradually reduced in length. Crucially, during this process we ensure that the angle between the two sides (θ_3) also remains constant. The dimensionless chirality index of the triangle (Γ_{ijk}) can now be expressed in the following form:

$$\Gamma_{ijk} = \frac{1 - r^2}{1 + r^2 - 2r\cos(\theta_3)} + 2\left(r - \frac{1}{r}\right)\cos(\theta_3) \quad (14)$$

where $r = a_2/a_1$. As $r \to 0$ we can see that Γ_{ijk} diverges whenever $\cos(\theta_3)$ is non-zero. The underlying reason for this behaviour is that, as the length of side a_2 reduces, eventually the angle of the triangle opposite side a_1 will become obtuse. This results in $\Gamma_1 > 1$ for vertex 1, and as side a_2 continues to decrease further in length, Γ_1 will then tend to infinity. This problem can only be eliminated if the mirror plane through each vertex also passes through the body of the triangle (as it does in the perpendicular bisection method of the previous section). Then the modulus of the dimensionless chirality index at any vertex $|\Gamma_i|$ can never exceed unity.

6. The angular bisection method

The perpendicular bisection method described in section 4 is not the only geometric configuration of high symmetry where the mirror plane is always guaranteed to pass through the body of the triangle. We can also choose a mirror plane that bisects the angle at any vertex of the triangle, as illustrated in figure 2(e). If we again calculate the difference in areas subtended by the triangle across this line as a fraction of the total area of the triangle we find that it has the following form:

$$\Gamma_1 = \frac{\Delta_R - \Delta_L}{\Delta_R + \Delta_L} = \frac{a_2 - a_3}{a_2 + a_3} \quad (15)$$

where Δ_L is the area to the left of the mirror plane (again as viewed from the vertex) and Δ_R is the area to the right. As before, we need to repeat the process for all three vertices in order to arrive at an expression that properly reflects the chirality of the triangle as a whole, rather than just the property of a single vertex. The dimensionless chirality index is then

$$\Gamma_{ijk} = \frac{a_1 - a_2}{a_1 + a_2} + \frac{a_2 - a_3}{a_2 + a_3} + \frac{a_3 - a_1}{a_3 + a_1}. \quad (16)$$

Inspection of equation (16) shows that Γ_{ijk} will always remain finite. In addition, when the length of any one side is zero, $\Gamma_{ijk} = 0$. Therefore, in addition to the perpendicular bisection method, we now have a second model for Γ_{ijk} that satisfies all of our initial conditions, including postulate 2.6 and lemma 2.9. If we define a triangle by three vectors, $\mathbf{r}_i$, $\mathbf{r}_j$ and $\mathbf{r}_k$, we can extend our model for chirality to any ensemble of N points as follows:

$$K = \frac{1}{4}\sum_{i=1}^{N}\sum_{j=1}^{N}\sum_{k=1}^{N} m_i m_j m_k \frac{|\mathbf{r}_{ij}| - |\mathbf{r}_{ik}|}{|\mathbf{r}_{ij}| + |\mathbf{r}_{ik}|}(\mathbf{r}_{ij} \times \mathbf{r}_{ik}). \quad (17)$$

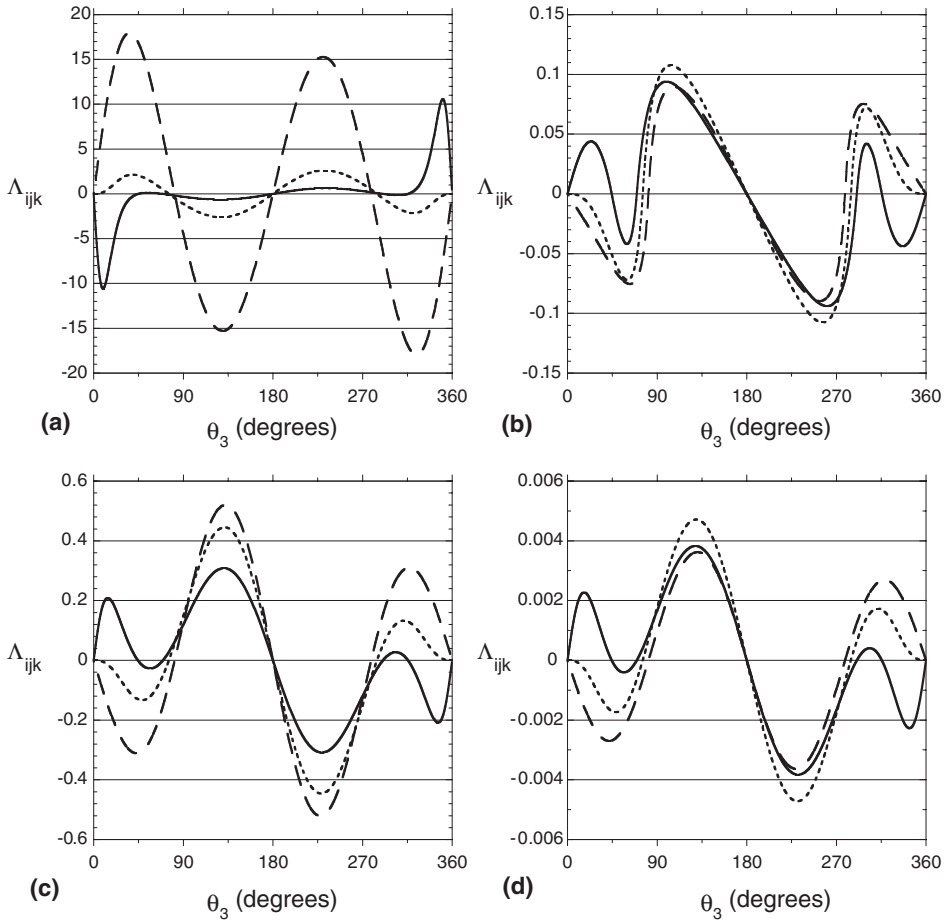

Figure 3. Plots of the specific chirality index (Λ_{ijk}) of a triangle as a function of the angle θ_3 between two adjacent sides (a_1 and a_2) for four different chirality models: (a) the Osipov model (equation (1)); (b) the perpendicular bisection method (equation (10)); (c) the perpendicular intercept method (equation (13)); (d) the angular bisection method (equation (17)). In each case the numerical calculation is performed for three different ratios of sides $r = a_2/a_1$: (i) $r = 0.3$ (dotted curve); (ii) $r = 0.5$ (full curve); (iii) $r = 0.7$ (broken curve). The values for Λ_{ijk} are normalized for the case $a_1 = 1$.

Interestingly, equation (17) is invariant under any interchange of subscript i, j or k. Therefore the user does not need to consider the cyclic ordering to ensure that the vertices i, j and k are arranged in a clockwise fashion, as this is already accounted for in the equation. Consequently, it is a trivial exercise to rewrite equation (17) in integral form:

$$K = \tfrac{1}{4}\int_{\mathbf{r}_i}\int_{\mathbf{r}_j}\int_{\mathbf{r}_k} \rho(\mathbf{r}_i)\rho(\mathbf{r}_j)\rho(\mathbf{r}_k) \times \frac{|\mathbf{r}_{ij}| - |\mathbf{r}_{ik}|}{|\mathbf{r}_{ij}| + |\mathbf{r}_{ik}|}(\mathbf{r}_{ij} \times \mathbf{r}_{ik})\, \mathrm{d}^2\mathbf{r}_k\, \mathrm{d}^2\mathbf{r}_j\, \mathrm{d}^2\mathbf{r}_i. \quad (18)$$

In the following section we will compare the behaviour of the three models described in sections 4–6 by applying them to a number of simple geometric structures.

7. Results

In order to explore the behaviour of the different chirality models we have described in this paper, it is instructive to first consider the behaviour of each for the case of a simple triangle of points, such as that depicted in figure 1. We have therefore calculated the specific chirality index (Λ_{ijk}) for this system using each of the models described in sections 4–6 and compared them with the theory of Osipov *et al* (equation (1)). In order to explore the parameter space of this three-particle system, we considered the behaviour of Λ_{ijk} for three different ratios of side ($r = a_2/a_1$) as the included angle of the triangle (θ_3) was allowed to vary. The results of this investigation are shown in figure 3 and are normalized for the case where the side a_1 of the triangle had unit length.

As expected, all four models exhibit behaviour that is consistent with postulate 2.7 and lemma 2.8. The specific chirality index is zero when the triangle is isosceles (i.e. when $a_3 = a_2$ or $a_3 = a_1$) or when the three points are co-linear ($\theta_3 = 0°, 180°, 360°$). It should be noted, however, that, when $r = 0.5$, the condition $a_3 = a_2$ occurs simultaneously with the three points being co-linear and so there is a point of inflection at $\theta_3 = 0°$. When $r < 0.5$, only the equality $a_3 = a_1$ can be satisfied and so there is only a single crossing of the abscissa axis in this case.

Despite the striking similarities of the four models illustrated in figure 3, they do also appear to exhibit some profound differences. The most obvious one is the sense of chirality in figure 3(a), which is opposite to that seen for the other three models. This, though, is merely an artefact of the way the initial sign convention for chirality in each model

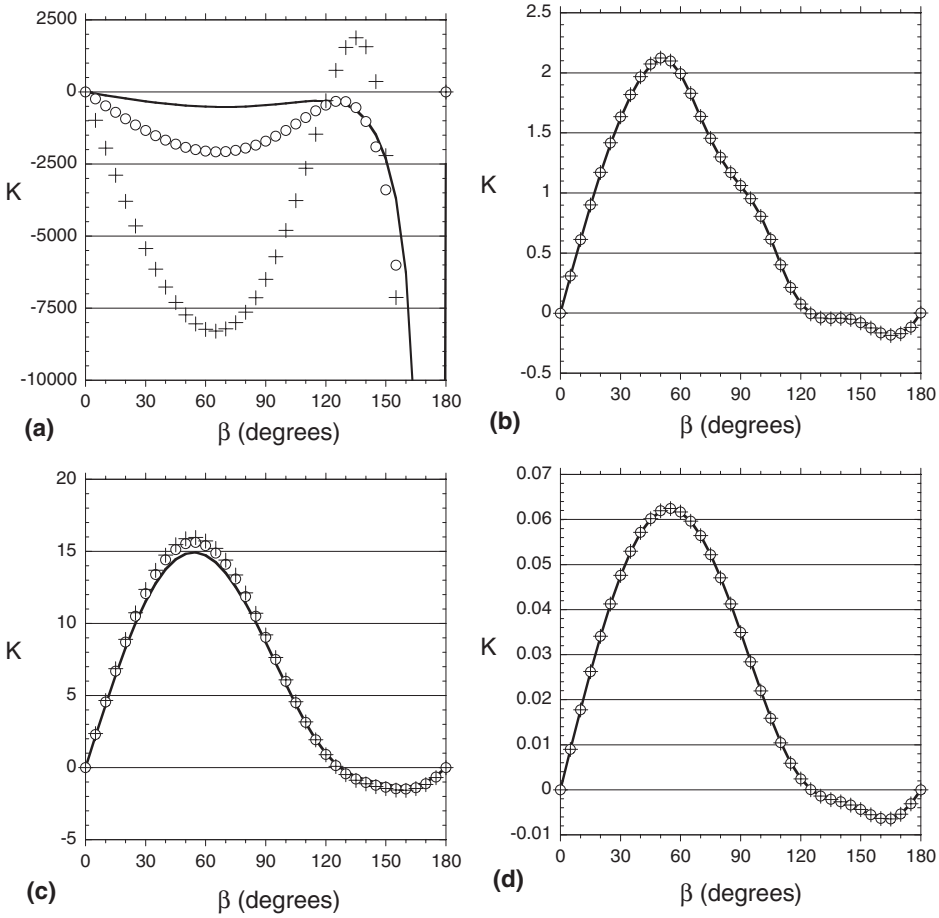

Figure 4. Plots of the chirality index (K) for the single gammadion illustrated in figure 5(a) as a function of bending angle β for four different chirality models: (a) the Osipov model (equation (1)); (b) the perpendicular bisection method (equation (10)); (c) the perpendicular intercept method (equation (13)); (d) the angular bisection method (equation (17)). In each case the numerical calculation is performed for three different pixel sizes: (i) $0.1L$ (full curve); (ii) $0.05L$ (○); (iii) $0.025L$(+). The values for K are normalized for the case $L = 1$.

is arbitrarily chosen and is therefore of no real consequence. More significant is the fact that the magnitude of the chirality in figure 3(a) decreases as r increases. A similar behaviour is seen in figure 3(c), but in figures 3(b) and (d) the opposite effect is observed. This is a direct consequence of the fact that the models illustrated in figures 3(b) and (d) (the perpendicular bisection model and the angular bisection model, respectively) both satisfy lemma 2.9, while the other two models do not. In figures 3(a) and (c), Λ_{ijk} diverges as a_2 (and hence r) tends to zero: in figures 3(b) and (d) it converges towards zero. This behaviour has profound implications for the integrability of each of the various models, as will be illustrated in figure 4. However, the divergent behaviour in figures 3(a) and (c) also implies that these two models will violate postulate 2.3, because the chirality index will not generally be continuous or single-valued as $r \to 0$.

In order to examine the integrability of the various models studied in figure 3, we used each model to calculate the chiral index, K (see figure 4), of a gammadion-shaped element of similar design to those we have investigated experimentally [2, 3]. In each case the chirality index was calculated as a function of the bending angle (β) of the gammadion arms (see figure 5(a) for an illustration of the gammadion geometry). The numerical integration was performed by pixelating the structure and summing over all permutations of pixels in accordance with postulate 2.1. In order to evaluate the numerical accuracy of this technique we repeated this operation for three different pixel sizes corresponding to 10, 20 and 40 pixels per length L of the arm.

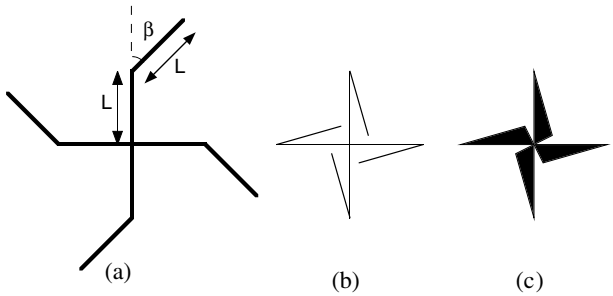

Figure 5. (a) A schematic diagram of the gammadion design used to compare the different chirality measures in figure 4. L is the arm length and β is the bending angle. (b) A schematic illustration of a gammadion with large bending angles. (c) An illustration of how the gammadion with large bending angles in (b) may appear to be similar to one constructed from four very thin, slightly offset, isosceles triangles. The result is that the direction of the chirality for large bending angles will be reversed compared to that observed for smaller bending angles.

In the case of the angular bisection method, increasing the number of pixels had little or no effect on the calculated chirality index (see figure 4(d)). The same was true for the perpendicular bisection method (figure 4(b)). Both of these chirality models appear, therefore, to be convergent and fully integrable. In the case of the Osipov model (figure 4(a)), however, we see that the calculated chirality index diverges significantly as the number of pixels increases and the distance between them decreases. The perpendicular bisection method (figure 4(c)) showed a similar type of behaviour, but the degree of divergence was not as great. This is consistent with the behaviour of Γ_{ijk} in equation (14) as the length of one side of the triangle tends to zero. The pole in Γ_{ijk} leads to a logarithmic divergence in K as $r \to 0$. In the case of the Osipov model, Γ_{ijk} contains a multiple pole of order r^{-4}, and hence the degree of divergence in K is much greater.

One of the unexpected results of the integration of the gammadion structure was the observation that the maximum chirality occurs for a bending angle $\beta \sim 55°$, irrespective of the model used. This peak in chirality occurs at an angle that is significantly less than the 90° one might intuitively expect. It should be noted, though, that this is consistent with our experimental observations [2, 3], which have already shown that gammadions with bending angles of 45° exhibit a much greater change on the polarization state of diffracted light than gammadions with bending angles of 90° or 135°. Whether this is evidence of a real correlation between the chirality index and the optical activity of the structure, or whether it is just coincidence, is still being investigated. More surprising, though, is the change in the sense of chirality of the gammadions as the bending angle approaches 180°. This behaviour is predicted by all three of our chirality models (figures 4(b)–(d)). We have attempted to explain this in figure 5(b) by showing how, in these circumstances, the two segments of each arm can appear to merge together and approximate to a very long, thin, isosceles triangle (figure 5(c)). The offset of these triangles then determines the new sense of chirality which, while relatively small in magnitude, is nevertheless in the opposite sense to the chirality index measured at smaller bending angles. Whether such effects are strong enough to be seen experimentally remains to be determined.

It is clear from the results shown in figures 3 and 4 that both the perpendicular bisection model and the angular bisection model satisfy the full list of criteria set out in section 2. Both models are fully integrable and scalable and both give similar predictions for the behaviour of the chirality index in a variety of simple structures. The only significant differences between the two models are the magnitude of the chirality and the angle at which the chirality index reaches a maximum. For the perpendicular bisection model, this appears to occur when θ_3 is almost a right angle and is preceded by an extremely rapid change in the chirality index as Λ_{ijk} changes sign, while for the angular bisection model the peak chirality occurs at $\theta_3 \sim 130°$.

There is one regime, however, where the behaviour of the two models is completely different. If we consider the behaviour of both models for the case of infinite triangles we find that they give some interesting results. Figure 6 shows the behaviour of the chirality index (K_{ijk}) of the triangle in figure 1 using the angular bisection model as side a_2 and angle

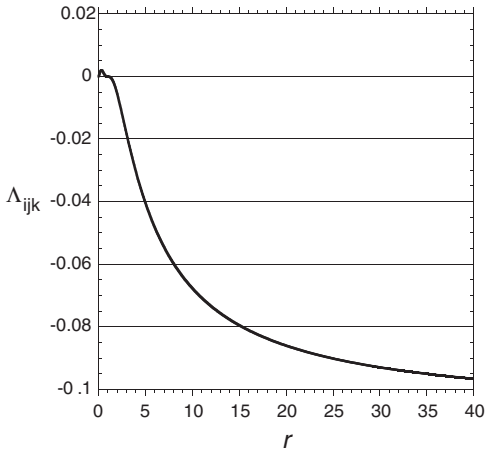

Figure 6. The specific chirality index (Λ_{ijk}), defined by the angular bisection method, for the triangle in figure 1 as a function of the ratio of sides ($r = a_1/a_2$), when the included angle (θ_3) is kept constant. The values for Λ_{ijk} are normalized for the case $a_2 = 1$ and $\theta_3 = 60°$.

θ_3 are kept constant but side a_1 is varied in length over the range $0 < a_1 < \infty$. Surprisingly, as $a_1 \to \infty$ we find that the chirality index remains finite. In fact, we find that the specific chirality index has the limiting form

$$|\Lambda_{ijk}| < \tfrac{1}{4} a_2^2 \sin(2\theta_3) \tag{19}$$

where a_2 is the shortest side of the triangle and θ_3 is the angle between the shortest side and the longest side. We can therefore conclude that, for triangles defined by three finite point masses, one at each vertex, only those for which all three sides of the triangle are infinite in length can have a chirality index which is itself infinite. This is in contrast to the perpendicular bisection model (section 4) where the dimensionless chirality index, Γ_{ijk}, has the limiting form of ± 1 (depending on whether θ_3 is obtuse or acute) as $a_1 \to \infty$ and therefore the specific chirality index, $\Lambda_{ijk} \to \infty$. These results are depicted graphically in figure 7, which shows how the three models formulated herein differ in the limit of convergent points. So, which model is correct?

Consider the following scenario. Suppose you are an observer standing on the point mass m_3 of the triangle in figure 1. As the side a_1 increases in length the point m_2 gradually disappears into the distance. Now ask yourself 'what is my perception of the magnitude of the chirality of this triangle?' One possible answer is that it is defined uniquely by the length of side a_2 and the angle θ_3 (or θ_2). The side a_1 is now so long that you cannot see its furthest end and it is now virtually parallel to side a_3. If side a_1 increases in length even more your perception of the chirality will remain unchanged even though the triangle is now even larger in area. To you, the observer, the side a_1 only defines a direction against which the rotation of side a_2 is measured. The sense and magnitude of the chirality appear only to depend on the size and orientation of the side a_2. The length of a_1 is irrelevant. It is therefore logical to conclude that the chirality index in this instance should be governed only by a_2 and θ_3 (as stated in equation (19)) and, because a_2 is finite, then the chirality index should also remain finite even as a_1 tends to infinity (as shown in figure 6).

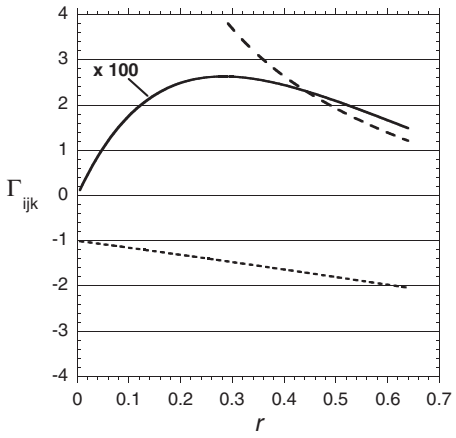

Figure 7. A plot of the dimensionless chirality index (Γ_{ijk}) for the triangle in figure 1 as a function of the ratio of sides $r(= a_2/a_1)$ for three different chirality models: (i) perpendicular bisection method (dotted curve); (ii) perpendicular intercept method (broken curve); (iii) angular bisection method (full curve). In all cases the included angle $\theta_3 = 120°$. For clarity, the data illustrating Γ_{ijk} for the angular bisection method (full curve) are scaled by a factor of 100.

Now look at the same scenario, but from a different perspective. Suppose you observe the triangle from above. As the side a_1 increases in length you will need to move further and further away from the triangle in order to maintain the whole of the triangle in your field of view. As you do so side a_1 will thus appear unchanged in size, but side a_2 will become smaller and smaller and its size will gradually tend to zero. Eventually point m_1 will merge with point m_3 and they will appear coincident. As an observer, what you are examining is the behaviour of the dimensionless chirality index (Γ_{ijk}) in the limit of convergent points. The above analysis suggests that the dimensionless chirality index (Γ_{ijk}) should tend to zero in this case, just as the chirality index (K_{ijk}) does (see lemma 2.9). This, then, is our final condition for two-dimensional chirality.

Postulate 7.1. If any two points of a triangle are coincident in space then the dimensionless chirality index must be zero. This implies that $\Gamma_{ijk} \to 0$ as $|\mathbf{r}_{ij}| \to 0$, where $|\mathbf{r}_{ij}|$ is the length of any side of the triangle.

Of the three models outlined above, only the angular bisection model satisfies postulate 7.1 (see figure 7). In the limit of converging points Γ_{ijk} diverges for the perpendicular intercept model, thus leading to a discontinuity in Λ_{ijk} as the points finally merge, in violation of postulate 2.3. In the case of the perpendicular bisection model, Γ_{ijk} converges to a finite but non-zero limit. Thus there is a discontinuity in Γ_{ijk} but not in Λ_{ijk}. This inevitably leads to $\Lambda_{ijk} \to \infty$ as $a_1 \to \infty$ in this case. Only the angular bisection model fully satisfies postulate 7.1 with both Γ_{ijk} and Λ_{ijk} being finite and continuous in the converging point limit, even when the area of the triangle is infinite (as illustrated in figure 6).

It should be pointed out that, while we have tried to argue the case for postulate 7.1, we have not proved it conclusively. The final answer may ultimately lie in the behaviour and predictions of each model for infinite systems, particularly fractal and periodic systems. In such systems the ultimate test will be whether it is possible to define a finite chirality measure in an infinite system, such as a finite chirality measure per unit cell for an infinite periodic structure.

8. Summary

In attempting to derive a measure of two-dimensional chirality our aim has been to construct a theory that is scalable, integrable and simple to implement for any 2D density distribution. To this extent the theory we have proposed in section 6 satisfies all these considerations. We started by defining a framework of rules that our theory should comply with (see section 2) and then constructing a model for that theory based on the principles of symmetry and area (section 3). Our ten tenets of two-dimensional chirality then allowed us to propose and test three different models for a 2D chirality measure. Each model was constructed by combining basic principles of group theory and symmetry (using techniques similar to those used by other workers [9]) with the concept of the overlap integral [10] and applying them to the simplest possible element of any two-dimensional system, the triangle. The only difference between our three models was the initial symmetry operation used in each case to generate the overlap between the original triangle and its enantiomer. We then compared our three models by testing them against our 'ten commandments' of chirality to see which, if any, satisfied all of the criteria. As was illustrated in the previous two sections, the angular bisection model was found to be the most successful although, depending on the validity or otherwise of postulate 7.1, the perpendicular bisection model may yet prove a suitable candidate.

It is clear that the theory (or theories) expounded herein represents a significant advance in this area, not least because it appears to concur with recent experimental results [2, 3]. It also has the added advantage that it appears to unite aspects of other theoretical approaches, such as group theory [9], overlap integrals [10] and the summation rules for large systems [11], into a single unified framework. This unification may suggest an underlying universality.

Central to our search for a universal chirality measure has been the development of a list of rules or tenets that underpin the form of chirality in two-dimensional systems. Implicit in these rules is the nature of the scaling behaviour of our system and its dimensions (see postulate 2.5). Because we assumed an initial scaling for each triangle that was proportional to its area (see lemma 2.4 and postulate 2.5), and because of the incorporation of the concept of mass (lemma 2.2), the chirality index in our model has dimensions of $(\text{mass})^3 \times (\text{area})$ and hence scales as α^8, where α is the magnification factor. This has implications for measuring the chirality index of infinite periodic systems and other infinitely tiled systems (such as Penrose tiling). In such systems the elemental chirality will scale with the number of tiles but the structural chirality may scale much faster, depending on the asymptotic behaviour of the chirality index of infinite triangles. Potentially there is a conflict here that poses the question of how one defines a finite chirality measure in such infinite systems and how one distinguishes between local and non-local chirality. The validity or otherwise of postulate 7.1 could play a vital role here in resolving these issues. Clearly, the issue of chirality in infinite systems is one that deserves greater attention and is an issue that we hope to address further in the future.

Acknowledgment

This work has been supported by the Engineering and Physical Sciences Research Council (UK).

References

[1] Hecht L and Barron L D 1994 *Chem. Phys. Lett.* **225** 525
[2] Potts A, Papakostas A, Zheludev N I, Coles H J, Greef R and Bagnall D M 2002 *Mater. Res. Soc. Symp. Proc.* **722** 293
[3] Papakostas A, Potts A, Bagnall D M, Prosvirnin S L, Coles H J and Zheludev N I 2003 *Phys. Rev. Lett.* **90** 107404
[4] Arnaut L R and Davis L E 1995 *Proc. Int. Conf. on Electromagnetics in Advanced Applications (Turin, Italy 1995)* pp 381–4
[5] Attard G A 2001 *J. Phys. Chem.* B **105** 3158
[6] Sholl D S, Asthagiri A and Power T D 2001 *J. Phys. Chem.* B **105** 4771
[7] Weinberg N and Mislow K 1993 *J. Math. Chem.* **14** 427
[8] Zimpel Z 1993 *J. Math. Chem.* **14** 451
[9] Zabrodsky H and Avnir D 1995 *J. Am. Chem. Soc.* **117** 462
[10] Buda A B, auf der Heyde T P E and Mislow K 1991 *J. Math. Chem.* **6** 243
[11] Osipov M A, Pickup B T, Fehervari M and Dunmur D A 1998 *Mol. Phys.* **98** 283
[12] Kelvin W T 1904 *Baltimore Lectures on Molecular Dynamics and the Wave Theory of Light* (London: C J Clay) pp 439, 618
[13] Barron L D 1994 *Chem. Phys. Lett.* **221** 311
[14] Le Guennec P 2000 *J. Math. Phys.* **41** 5954
[15] Solymosi M, Low R J, Grayson M and Neal M P 2002 *J. Chem. Phys.* **116** 9875
[16] Osipov M A, Pickup B T and Dunmur D A 1995 *Mol. Phys.* **84** 1193